

The Green Location-Routing Problem

Okan Dukkanci[†]

Bahar Y. Kara^{†*}

Tolga Bektaş[‡]

[†]*Department of Industrial Engineering
Bilkent University, 06800 Ankara, Turkey*

[‡]*University of Liverpool Management School,
University of Liverpool, Liverpool L69 7ZH, United Kingdom*

Abstract

This paper introduces the Green Location-Routing Problem (GLRP), a combination of the classical Location-Routing Problem (LRP) and the Pollution-Routing Problem (PRP). The GLRP consists of (i) locating depots on a subset of a discrete set of points, from where vehicles of limited capacity will be dispatched to serve a number of customers with service requirements, (ii) routing the vehicles by determining the order of customers served by each vehicle and (iii) setting the speed on each leg of the journey such that customers are served within their respective time windows. The objective of the GLRP is to minimize a cost function comprising the fixed cost of operating depots, as well as the costs of the fuel and CO₂ emissions. The amount of fuel consumption and emissions is measured by a widely used comprehensive modal emission model. The paper presents a mixed integer programming formulation and a set of preprocessing rules and valid inequalities to strengthen the formulation. Two solution approaches; an integer programming based algorithm and an iterated local search algorithm are also presented. Computational analyses are carried out using adaptations of literature instances to the GLRP in order to analyze the effects of a number parameters on location and routing decisions in terms of cost, fuel consumption and emission. The performance of the heuristic algorithms are also evaluated.

Keywords. vehicle routing; depot location; fuel consumption; CO₂ emissions; integer programming.

*Corresponding author: bkara@bilkent.edu.tr

1 Introduction and Background

Recent decades have seen a growing interest in green logistics, which can broadly be defined as planning and execution of logistics activities in a more environmentally friendly way by considering external factors such as waste, noise, energy usage and Greenhouse Gas (GHG) emissions. “Green routing” is a concept first introduced by Kara et al. (2007) by observing the fact that “cost” is not usually directly proportional to distance traveled but also the load of the vehicle. Palmer (2007) study the integration of vehicle routing and CO₂ emissions. Bektaş and Laporte (2011) introduce the Pollution-Routing Problem (PRP) with a more accurate fuel consumption model that considers speed and load as decisions. Variants of the PRP have since been studied, such as time-dependency (Jabali et al., 2012), with backhauling (Ubeda et al., 2011), with pickup and delivery (Oberscheider et al., 2013) and with inventory considerations (Mirzapour Al-e hashem and Reikik, 2014). For comprehensive survey on green routing and green logistics, we refer the reader to Sbihi and Eglese (2010), Dekker et al. (2012), Lin et al. (2014), Demir et al. (2014*b*) and Eskandarpour et al. (2015), and to Ubeda et al. (2011), Figliozzi (2011) and Varsei and Polyakovskiy (2017) for case studies.

Table 1 summarizes the relevant literature of “green routing” problems and compares them with our study based on the following seven factors: (i) the number of objective functions (single or multiple), (ii) type of emission model used, (iii) the proposed solution approaches (exact or heuristic), (iv) whether these studies consider time windows or not, and (v,vi,vii) whether speed, location and routing are considered as decisions or not.

Table 1: Features of “green routing” problems

Reference	Objective	Emission Model	Solution Method	Time Windows	Speed	Location	Routing
Kara et al. (2007)	Single	Factor	Exact				✓
Palmer (2007)	Single	IFCM	Heuristic		✓		✓
Figliozzi (2010)	Multi	MEET	Exact & Heuristic	✓			✓
Figliozzi (2011)	Multi	MEET	Exact & Heuristic	✓	✓		✓
Bektaş and Laporte (2011)	Single	CMEM	Exact	✓	✓		✓
Demir et al. (2012)	Single	CMEM	Exact & Heuristic	✓	✓		✓
Jabali et al. (2012)	Single	MEET	Heuristic		✓		✓
Demir et al. (2014 <i>a</i>)	Multi	CMEM	Heuristic	✓	✓		✓
Qian and Eglese (2014)	Single	NAEI	Heuristic	✓	✓		✓
Our Study	Single	CMEM	Exact & Heuristic	✓	✓	✓	✓

IFCM: Instantaneous fuel consumption model

MEET: Methodology for calculation transportation emissions and energy consumption

NAEI: National atmospheric emissions inventory

(see Demir et al., 2014*b*, for a detailed description of these models)

The Location-Routing Problem (LRP) is a generalization of the vehicle routing problem that exploits the interdependency between the location decisions of facilities and routing decisions of vehicles, as it has been shown that making the two decisions independently can result in suboptimal solutions (Salhi and Rand, 1989). The basic LRP involves locating facilities and routing a fleet of vehicles from the

facilities to serve a given set of customers, with the aim of minimizing the cost of location and routing (see, e.g., Prodhon and Prins, 2014; Drexl and Schneider, 2015, for comprehensive surveys).

To the best of our knowledge, there are only a few studies that consider environmental impacts within the LRP literature. The first one is by Govindan et al. (2014), who describe a bi-objective two echelon LRP with time windows which arises in a perishable food supply chain network with manufacturers, distribution centers and retailers. The two objectives are to minimize the total cost and to minimize the environmental impact. They propose a multiobjective hybrid approach by combining multiobjective particle swarm optimization and an adaptation of a multiobjective variable neighborhood search. The second study is by Koç et al. (2016) in which the authors analyze the impact of location, fleet composition and routing on emissions in urban freight transportation. The authors present a location-routing problem with heterogeneous fleet of vehicles in a city logistics concept, which use the comprehensive modal emission model (CMEM) proposed by Scora and Barth (2006), Barth et al. (2005), Barth and Boriboonsomsin (2008) to calculate emission. Based on city logistics concepts, cities are divided into three different speed zones and vehicle speed is considered to be fixed in each speed zone. The objective is to minimize the total cost which includes those of depots, operating vehicles, fuel consumption and CO₂ emissions. The authors utilize an adaptive large neighborhood search algorithm to solve the problem and to conduct sensitivity analyses. Toro et al. (2017) study a bi-objective green capacitated location-routing problem with two objective functions that minimize the operational cost and fuel consumption and CO₂ emission. The authors use the ϵ -constraint method to solve the corresponding bi-objective mathematical model. Tricoire and Parragh (2017) present a green city hub location routing problem with heterogeneous fleet and with two objectives; to minimize the total cost and minimize CO₂ emissions. The authors develop a decomposition approach that first generates vehicle routes which are used for a set covering model. The authors test their algorithm on instances obtained from industrial partners in Austria that include 22 hubs, 898 or 1635 customers, and two or seven vehicle types. The authors explore the trade-offs between the amount of pollution and the cost in investing in facilities.

In a recent study, Khoei et al. (2017) propose a green Weber problem and its time-dependent version, where the authors combine the location decision of a single facility and the speed decisions of the vehicles sent to customers to minimize the total amount of CO₂ emissions. This is the first study that integrates vehicle speeds and time windows in a location problem, although it does not consider vehicle routes.

Table 2 presents features of the existing “green location-routing and green location” problems and provides a comparison between them and our study.

Similar to other related studies (Bektaş and Laporte (2011), Demir et al. (2012), Demir et al. (2014a))

Table 2: Features of “green location-routing and green location” problems

Reference	Objective	Emission Model	Solution Method	Time Windows	Speed	Location	Routing
Govindan et al. (2014)	Multi	Factor	Heuristic	✓		✓	✓
Koç et al. (2016)	Single	CMEM	Exact & Heuristic			✓	✓
Toro et al. (2017)	Multi	Macroscopic	Exact			✓	✓
Tricoire and Parragh (2017)	Multi	Factor	Exact & Heuristic			✓	✓
Khoei et al. (2017)	Single	CMEM	Exact	✓	✓	✓	
Our Study	Single	CMEM	Exact & Heuristic	✓	✓	✓	✓

that use CMEM as the emission model, we also treat speed and load as decision variables in order to estimate the emissions more accurately. This makes our study different to other studies that study a location-routing problem with environmental concerns.

Although not many scientific studies yet exist on the LRP with an explicit consideration of fuel consumption and emissions, recent developments in practice suggest that this is a growing area of attention, particularly in cargo and fast-moving consumer goods (FMCG) industries. Unilever, for example, who operates in the FMCG industry, has adopted a new Transport Management System since 2012, which optimizes transport flows between suppliers, factories, warehouses and retailers, using a new network structure. Increasing transport and fuel efficiency and reducing emissions are the main drivers behind this system (Unilever, 2017). Similar initiatives have been put in place by other companies, such as UPS who achieved a reduction of 25,000 metric tonnes of CO₂ through optimizing their network in 2015 (UPS, 2015), and FedEx who invested in an EarthSmart program since 2010 to reduce transportation related emissions by optimizing vehicle loads and routes (FedEx, 2011). FedEx also ask their drivers to apply idle reduction and speed control techniques to reduce fuel consumption (FedEx, 2016). DHL opened a new logistics center in Milan to reduce emissions as part of network design in a GoGreen environmental protection program. This new center, which is located in a strategic region of Milan that can be combined with air and sea transportation, uses 120 trucks to deliver 810,000 tons of goods per year. A recent press release indicates that the new DHL center has resulted in an “estimated reduction of facility and transport CO₂ emissions of 18 per cent at the new site. 13 per cent of which can be traced back to an improved road network and a reduction of both transit time and the average fuel consumption” (DHL, 2012). Recently, DHL has made another significant investment by opening a logistics hub in Milan Malpensa Airport which transports 60% of Italian goods and is the sixth largest cargo airport in Europe. One of the company executives emphasizes that the company will focus on the environmental sustainability for this new hub, which requires an investment of €350m over the next five years (DHL, 2016). These recent initiatives serve to illustrate the growing importance of the need to optimize the network structure to be able to reduce environmental externalities, which include decisions concerning routing and location.

Another application area of the GLRP has emerged due to recent developments in on-road vehicle technologies. One example where this is being put in practice is a European Commission research project known as Sartre - Safe Road Trains for the Environment. In this application, a lead vehicle (usually a truck) travels ahead of a platoon formed by other semi-autonomous vehicles, which all follow and travel at the same speed as the lead vehicle. The ability to maintain a constant speed allows to achieve reductions in congestion, fuel consumption and accidents. Trials of the road train technology were successfully held in Sweden (Ward, 2011) and Spain (Volvo, 2012). Another more recent practice is the use of autonomous vehicles. These type of vehicles also maintain a relatively constant speed on the road compared to conventional vehicles. Recently, Daimler AG, an automotive corporation that owns Mercedes-Benz, launched two autonomous trucks; Mercedes-Benz Future Truck 2025 (Wysocky, 2014) and Freightliner Inspiration Truck (Linshi, 2015). Although these vehicles are still being trialled, they are expected to be driven on the roads in the near future (Dougherty, 2017). Consequently, most of the leading cargo companies have started to consider using such new technologies in their delivery operations; DHL published a report on self-driving vehicles in logistics based on its benefits and applications (DHL, 2014), US Postal Service is planning to make deliveries using self-driving mail trucks within seven years (Marshall, 2017), FedEx is also interested in autonomous vehicles and is collaborating with the manufacturers, Daimler and Volvo (Woyke, 2017), and Amazon formed a team to study self-driving vehicles (Stevens and Higgins, 2017).

In this study, we introduce the Green Location-Routing Problem (GLRP), an extension of the LRP that explicitly accounts for fuel consumption and CO₂ emissions, the amount of which is measured by a widely used comprehensive modal emission model (CMEM). The GLRP consists of locating depots on a subset of a discrete set of points, from where vehicles of limited capacity will be dispatched to serve a number of customers with service requirements, and routing the vehicles by determining the order of customers served by each vehicle and the speeds on each leg of the journey, such that customers are served within their respective time windows and vehicle capacities are respected. The objective is to minimize a total cost function comprising depot, fuel and emission costs. As for the network, we assume a single echelon structure including the depot(s) and the customers.

The contributions of this paper along its structure are as follows: (i) we formally define the GLRP, (ii) we propose a mixed integer linear programming formulation for the GLRP, (iii) we strengthen the formulation by a set of preprocessing rules and valid inequalities, all of which are detailed in Section 2, (iv) we present two solution algorithms; one is to solve small-sized GLRP instances in reasonable times to near-optimality, and the other to efficiently solve large-sized GLRP instances, both of which are explained in Section 3, and (v) we conduct extensive computational analyses on the GLRP to quantify

the benefit of the location decisions on internal (operational) and external (environmental) costs, and to evaluate the performance of the heuristic algorithms detailed in Section 4. Conclusions are given in Section 5.

2 Problem Description and Formulation

The GLRP is defined on a complete directed graph $G = (N, A)$ where $N = \{1, \dots, n\}$ denotes the set of nodes representing both the set of customers and the potential sites for a total of p depots to be located, and $A = \{(i, j) : i, j \in N, i \neq j\}$ is the set of arcs. The fixed cost of operating a depot at node $i \in N$ is denoted by c_i . A fleet of m identical vehicles, each with capacity C serves the customers across the p depot(s). The distance on arc $(i, j) \in A$ is denoted by d_{ij} . Each customer i has a nonnegative demand q_i . The service time and time windows at node $i \in N$ are denoted by s_i and $[l_i, u_i]$, respectively. If a vehicle arrives at customer i before l_i , it waits until l_i and then service starts. The minimum and maximum speed limits for vehicles are denoted by v^l and v^u , respectively. The unit combined fuel consumption and emission cost is denoted by e .

2.1 Calculating fuel consumption and emissions

The CMEM was proposed by Scora and Barth (2006), Barth et al. (2005), Barth and Boriboonsomsin (2008) in order to estimate fuel consumption for heavy-goods vehicles. Since emissions are directly related to fuel consumption, one can easily calculate the amount of emissions when the fuel consumption is known. Compared to other microscopic emission models in the literature, it requires more detailed vehicle specific parameters such as the engine friction coefficient and the vehicle engine speed.

Based on the CMEM, the fuel consumption rate can be calculated as $F_r = \xi(K\Upsilon V + P/\eta)/\kappa$ in liters/second (L/s) where ξ is the fuel-to-air mass ratio, K is the engine friction factor, Υ is the engine speed, V is the engine displacement (in L), η is the efficiency parameter for diesel engines and κ is the heating value of a typical diesel fuel. Furthermore, $P = P_{tract}/n_{tf} + P_{acc}$ is the second-by-second engine power output (in kW), where n_{tf} is the vehicle drive train efficiency that relates to the overall efficiency of all components transmitting the engine power to the wheels, and P_{acc} is the engine power demand associated with running losses of the engine and the operation of vehicle accessories such as air conditioning usage. P_{tract} is the total tractive power requirement (in kW) and it can be calculated as follows:

$$P_{tract} = (Ma + Mg \sin \theta + 0.5C_d \rho S v^2 + Mg C_r \cos \theta) v / 1000,$$

where M is the total weight of the vehicle (in kg) including the empty vehicle weight ω and weight of

the goods carried, a is the instantaneous acceleration (in m/s^2), g is the gravitational constant (in m/s^2), θ is the road angle, C_d is the coefficient of aerodynamic drag, ρ is the air density (in kg/m^3), S is the frontal surface area (in m^2), v is the vehicle speed (in m/s) and C_r is the coefficient of rolling resistance.

To simplify the above formulation, some new parameters are used as follows: $\lambda = \xi/\kappa\psi$ where ψ is the conversion factor of fuel, $\gamma = 1/1000n_{tf}\eta$, $\alpha = a + g\sin\theta + gC_r\cos\theta$ is a vehicle-arc specific constant and $\beta = 0.5C_d\rho S$ is a vehicle-specific constant. With these new parameters, the total fuel consumption F (in L) for a vehicle traversing a road segment of d units (in m) at a constant speed v (in m/s) can be given as follows:

$$F = \alpha\lambda\gamma dM + \lambda\gamma d\beta v^2 + \lambda K\Upsilon V d/v.$$

As it can be seen from the expression above, the CMEM consists of three modules, namely the weight module (shown by $\alpha\lambda\gamma dM$), the speed module (defined by $\lambda\gamma d\beta v^2$) and the engine module (expressed by $\lambda K\Upsilon V d/v$). These three modules are explicitly included in the objective function of the mathematical model in the following section.

2.2 An Integrated Model of Location, Routing, Fuel Consumption and Emissions

In this section, we propose a mixed integer programming formulation for the GLRP which is based on the model developed by Bektaş and Laporte (2011). The decision variables are defined as follows: A binary variable x_{ij}^k equals 1 if a vehicle that is assigned to depot $k \in N$ travels on arc $(i, j) \in A$, and 0 otherwise. If the customer at node $i \in N$ is assigned to a depot at node $k \in N$, then a binary variable y_{ik} equals 1, and 0 otherwise. The service start time at node $j \in N$ is denoted by a continuous nonnegative variable t_j . Similarly, a continuous nonnegative variable f_{ij} represents the total amount of flow on arc $(i, j) \in A$.

As the vehicle speed is a decision variable, some of the objective function components and constraints of the formulation will have non-linear terms due to the emission function used. To linearize these terms, we adapt the discretization technique applied for the PRP by Bektaş and Laporte (2011). To that end, a finite set $R = \{1, \dots, r, \dots\}$ of speed levels is defined where $r \in R$ corresponds to a fixed speed v^r . In order to include the speed decision into the model, a new binary variable, w_{ij}^{kr} , is introduced which takes the value of 1, if a vehicle allocated to depot $k \in N$ travels with a speed level $r \in R$ on arc $(i, j) \in A$, and 0 otherwise. A mathematical model of the GLRP is as follows:

Minimize

$$\sum_{k \in N} c_k y_{kk} \tag{1}$$

$$+e \sum_{(i,j) \in A} \left[(\alpha\gamma\lambda d_{ij}\omega \sum_{k \in N} x_{ij}^k) \right] \quad (2.1)$$

$$+(\alpha\gamma\lambda d_{ij} f_{ij}) \quad (2.2)$$

$$+(\beta\gamma\lambda d_{ij} \sum_{k \in N} \sum_{r \in R} (v^r)^2 w_{ij}^{kr}) \quad (2.3)$$

$$+(K\Upsilon V\lambda d_{ij} \sum_{k \in N} \sum_{r \in R} \frac{w_{ij}^{kr}}{v^r}) \quad (2.4)$$

subject to

$$\sum_{k \in N} y_{ik} = 1 \quad \forall i \in N \quad (3)$$

$$y_{ik} \leq y_{kk} \quad \forall i, k \in N \quad (4)$$

$$\sum_{k \in N} y_{kk} = p \quad (5)$$

$$\sum_{k \in N} \sum_{j \in N \setminus \{k\}} x_{kj}^k \leq m \quad (6)$$

$$\sum_{j \in N \setminus \{i\}} x_{ij}^k = y_{ik} \quad \forall i, k \in N : k \neq i \quad (7)$$

$$\sum_{j \in N \setminus \{i\}} x_{ji}^k = y_{ik} \quad \forall i, k \in N : k \neq i \quad (8)$$

$$\sum_{j \in N \setminus \{k\}} x_{jk}^k = \sum_{j \in N \setminus \{k\}} x_{kj}^k \quad \forall k \in N \quad (9)$$

$$\sum_{r \in R} \left(\frac{d_{kj}}{v^r} \right) w_{kj}^{kr} \leq t_j \quad \forall j, k \in N : k \neq j \quad (10)$$

$$t_i + s_i + \sum_{r \in R} \left(\frac{d_{ij}}{v^r} \right) w_{ij}^{kr} - (u_i + s_i)(1 - x_{ij}^k) \leq t_j \quad \forall (i, j) \in A, k \in N : k \neq i, j \quad (11)$$

$$\sum_{r \in R} w_{ij}^{kr} = x_{ij}^k \quad \forall (i, j) \in A, k \in N \quad (12)$$

$$l_j(1 - y_{jj}) \leq t_j \quad \forall j \in N \quad (13)$$

$$t_j \leq u_j(1 - y_{jj}) \quad \forall j \in N \quad (14)$$

$$\sum_{j \in N \setminus \{i\}} f_{ji} \leq \sum_{j \in N \setminus \{i\}} f_{ij} - q_i(1 - y_{ii}) + \sum_{k \in N} q_k y_{ii} \quad \forall i \in N \quad (15)$$

$$\sum_{j \in N \setminus \{i\}} f_{ij} \leq C(1 - y_{ii}) \quad \forall i \in N \quad (16)$$

$$f_{ij} \leq C \sum_{k \in N} x_{ij}^k \quad \forall (i, j) \in A \quad (17)$$

$$x_{ij}^k \in \{0, 1\} \quad \forall (i, j) \in A, k \in N \quad (18)$$

$$y_{ik} \in \{0, 1\} \quad \forall i, k \in N \quad (19)$$

$$w_{ij}^{kr} \in \{0, 1\} \quad \forall (i, j) \in A, k \in N, r \in R \quad (20)$$

$$t_j \geq 0 \quad \forall j \in N \quad (21)$$

$$f_{ij} \geq 0 \quad \forall (i, j) \in A. \quad (22)$$

The objective function consists of two components. The first, shown by (1), minimizes the fixed cost of operating depots. The second part shown collectively by (2.1)–(2.4) minimizes the total cost of fuel consumption and emissions estimated by CMEM described in Section 2.1. In particular, the first two components (2.1) and (2.2) represent the weight module of the emission model in which (i) the empty vehicle weight ω is represented by the load-independent component (2.1), and (ii) the weight of the load carried associated to the load-dependent component (2.2) is represented by the flow variable f . Components (2.3) and (2.4) calculate the fuel consumption and emissions due to the speed and engine

modules of the CMEM, respectively. Constraint (3) ensures that every customer is assigned to exactly one depot. Constraint (4) stipulates that if a depot is not opened at a node, then none of the customers can be assigned to the depot at that node. Constraint (5) sets the number of depots to be opened equal to p . Constraint (6) guarantees that at most m vehicles can be used to serve the customers. With constraints (7) and (8), it is ensured that if a customer is assigned to a specific depot, then a vehicle visits this customer before and after two other customers which are also assigned to this depot. Constraint (9) ensures that the number of vehicles that leave and that arrive at the depot is the same. Constraints (10)–(14) are related to time and speed. Constraint (10) calculates the arrival time of a vehicle at the first customer visited after leaving the depot. Constraint (11) calculates the arrival times of a vehicle at customers assigned to the same depot as the vehicle. Constraint (11) is an adaptation of the well known subtour elimination constraints proposed by Miller et al. (1960) and prohibit the formation of tours solely within customer nodes. With constraint (12), vehicles can use only one of the specified speed levels over an arc. Constraints (13) and (14) model the time window constraints for customers. These constraints also stipulate that, if a depot is located at a node j (i.e., $y_{jj} = 1$), then $t_j = 0$, indicating that the customer at node j is served immediately. Constraint (15) provides flow conservation between nodes except where a depot is opened. In particular, f_{ij} is the total amount of demand in the route until, but excluding, customer j , and where a customer at node k is not taken into account if k is selected as a depot. Constraints (16)–(17) collectively enforce the vehicle capacity constraints on the flow on each arc. Finally, constraints (18)–(22) are the domain constraints on the variables.

2.3 Preprocessing and valid inequalities

This section describes some preprocessing rules and valid inequalities to strengthen the formulation presented in the previous section, and to potentially reduce solution times to optimality.

We first present a couple of variable fixing rules for w_{ij}^{kr} variables, which we implement prior to solving the formulation:

- If $l_i + s_i + \frac{d_{ij}}{v^r} > u_j$, then $w_{ij}^{kr} = 0$
- If $\frac{d_{kj}}{v^r} > u_j$, then $w_{kj}^{kr} = 0$.

The first rule dictates that if the sum of the lower time limit l_i at node i , the travel time $\frac{d_{ij}}{v^r}$ between nodes i and j and the service time s_i at node i is greater than the upper time limit u_j at node j , then w_{ij}^{kr} is set equal to zero. The second preprocessing rule is a special case of the first one where j is the first customer after the depot.

Next, we describe several valid inequalities in order to strengthen the linear programming (LP) relaxation of the mathematical formulation in the expectation of reducing the CPU times. These inequalities narrow the solution space by eliminating some fractional solutions and can provide stronger lower bounds for the problem.

First, we consider two-node subtour breaking constraint proposed by Dantzig et al. (1954) in order to eliminate cycles between two customers and develop two different valid inequalities as shown below:

$$x_{ij}^k + x_{ji}^k \leq y_{ik} \quad \forall (i, j) \in A, k \in N : k \neq i, j \quad (\text{VI 1.1})$$

$$\sum_{k \in N \setminus \{i, j\}} (x_{ij}^k + x_{ji}^k) \leq \sum_{k \in N \setminus \{i, j\}} y_{ik} \quad \forall (i, j) \in A. \quad (\text{VI 1.2})$$

VI (1.1) and (1.2) ensure that if a customer is assigned to a specific depot, then this customer and any other customer assigned to the same depot can have a link between them in only one direction.

Second, we develop a flow based valid inequality, which ensures that the amount of flow on arc $(i, j) \in A$ is larger than the demand q_i of node $i \in N$, unless node i is selected as a depot.

$$q_i (\sum_{k \in N} x_{ij}^k - y_{ii}) \leq f_{ij} \quad \forall (i, j) \in A. \quad (\text{VI 2})$$

The valid inequality we propose next provides a lower bound on the number of vehicles required, which is derived from the ratio of the demand of all customers (excluding depots) to the vehicle capacity.

$$\left(\frac{\sum_{k \in N} q_k (1 - y_{kk})}{C} \right) \leq \sum_{k \in N} \sum_{j \in N \setminus \{k\}} x_{kj}^k. \quad (\text{VI 3})$$

Similar inequalities to VI 3 were first proposed by Achuthan et al. (2003) for a vehicle routing problem, and later adapted for a location-routing problem by Karaoglan et al. (2012). The last sets of inequalities are stronger versions of the time window constraints (13) and (14). These inequalities are the adapted versions of Bektaş and Laporte (2011) proposed for the PRP.

$$l_j (1 - y_{jj}) + \sum_{i \in N \setminus \{j\}} \sum_{k \in N \setminus \{i, j\}} \sum_{r \in R} \max(0, l_i - l_j + s_i + \frac{d_{ij}}{v^r}) w_{ij}^{kr} \leq t_j \quad \forall j \in N \quad (\text{VI 4.1})$$

$$t_j \leq u_j (1 - y_{jj}) - \sum_{i \in N \setminus \{j\}} \sum_{k \in N \setminus \{i, j\}} \sum_{r \in R} \max(0, u_j - u_i + s_j + \frac{d_{ji}}{v^r}) w_{ji}^{kr} \quad \forall j \in N. \quad (\text{VI 4.2})$$

(VI 4.1) implies that service of a customer at node $j \in N$ starts after either the customer's lower time limit (l_j) or the sum of the lower time limit (l_i) and service time (s_i) of a customer at node $i \in N$ that proceeds it, and the travel time ($\frac{d_{ij}}{v^r}$) between these two customers. Similarly, (VI 4.2) guarantees that service of a customer at node $j \in N$ starts before either the customer's upper time limit (u_j) or the time

that ensures that the next customer's $i \in N$ service starts before its upper time limit (u_i) at worst.

3 Heuristic Algorithms for the GLRP

In this section, we present two heuristic algorithms to solve the GLRP. Both algorithms first divide the GLRP into subproblems; namely, the Cumulative Location Routing Problem (CumLRP) and the Speed Optimization Problem (SOP), and solve each in a hierarchical manner. In particular, once the CumLRP is solved, the location of the depots and the routes of the vehicles are determined. The SOP is then solved using the routes of the vehicles in order to identify the optimum speeds for the vehicles. The solutions found by the algorithms are feasible for the GLRP since it satisfies all the constraints imposed by the GLRP formulation. We describe the two heuristic algorithms in more detail below.

3.1 Cumulative location-routing and speed optimization algorithm (CLRSOA)

The Cumulative location-routing and speed optimization algorithm (CLRSOA) works as follows; first, one of the CumLRP formulations that will be introduced in Section 3.1.1 is solved to optimality. During the optimization process, some feasible solutions are stored in the "solution pool". Based on the depot locations and vehicle routes, the SOP is solved by the Speed Optimization Algorithm (SOA) explained in Section 3.1.2 for each of the solutions in the pool. Then, a feasible solution with the lowest objective function value is selected as the solution of the CLRSOA.

Next, we will present the mathematical formulations and solution techniques for the two subproblems.

3.1.1 Cumulative location-routing problem

The CumLRP is a special case of the GLRP where the time window constraints are relaxed and where the speed-induced fuel consumption cost is not included in the objective function. In other words, the objective function only minimizes the weight-induced fuel consumption cost. Singh and Gaur (2017) introduce the Cumulative Vehicle Routing Problem, where only routing decisions are made and where a factor model is used to estimate fuel consumption instead of a microscopic emission model as in the CumLRP. To the best of our knowledge, the Cumulative Location-Routing Problem (CumLRP) has not yet been defined in the literature. The main difference between the CumLRP and the classical LRP is the objective function. The classical LRP minimizes the operational cost that is a function of the total distance traveled. In the CLRP, the operational cost depends on both the distance traveled and the load of the vehicle.

An integer programming formulation of the CumLRP can be derived by removing the speed related objective function components (2.3–2.4), as well as the speed and time related decision variables and constraints from the GLRP formulation (Constraints 10–14). The mathematical model of the CumLRP is as follows:

$$\begin{aligned} & \text{Minimize (1) + (2.1) + (2.2)} \\ & \text{subject to} \\ & (3)-(9), (15)-(19), (22). \end{aligned}$$

In addition to the above CumLRP formulation, we also propose a different version of the CumLRP formulation CumLRP' to diversify the solutions in the “solution pool”. In the CumLRP', we assume that the vehicles travel at the optimal speed v^* on each arc of the network, calculated as follows. The fuel consumption function $F(v, f)$, which depends on speed v and load f , can be written as

$$F(v, f) = (\alpha\gamma\lambda dw) + (\alpha\gamma\lambda df) + (\beta\gamma\lambda dv^2) + (K\Upsilon V\lambda d/v),$$

from which $v^* = \sqrt[3]{\frac{K\Upsilon V}{2\beta\gamma}}$ is obtained as the global minimizer. The objective function of the CumLRP' formulation is the same as that of GLRP when $v^r = v^*$ for all $r \in R$.

The main difference between the CumLRP and the CumLRP' formulations is that in the latter, we add the cost components (2.3)–(2.4) in the objective function with the assumption that the vehicles travel at the optimal speed v^* , which makes the optimal value of the CumLRP' formulation a valid lower bound for the corresponding GLRP.

To solve the CumLRP or CumLRP' formulations within the CLRSOA, we use three different solution strategies of the solver CPLEX to diversify the solutions in the “solution pool”. The first one is the default “dynamic search”, the second is “traditional branch and cut” without the cuts (pure branch and bound algorithm), and third, a cut-and-branch method using the second technique, but with some of the valid inequalities added at the root node.

3.1.2 Speed optimization problem

Once the location of depots and route of vehicles are known, the only remaining decision is the speed to be used over each arc so that time windows will be obeyed and the total ‘cost’, which is composed of speed-induced fuel consumption will be optimized. This second subproblem is the speed optimization problem introduced by Demir et al. (2012) for road transportation. Given a route and time windows for

each customer, the problem decides the vehicle speed on each arc of the route while minimizing the total cost including fuel consumption and driver cost. As the estimation of fuel consumption is non-linear, the authors presented a non-linear formulation.

Since we do not consider driver cost in the GLRP, we only minimize the fuel consumption in our version of the speed optimization problem. In addition, we do not need to decide on the vehicle speed for the arc between the last customer visited before the depot and the depot itself since the vehicles travel at the optimal speed v^* on this arc because there is no time related constraint for returning the depot. Based on these differences between the formulation proposed by Demir et al. (2012) and our version, we reformulate the corresponding speed optimization problem.

Speed optimization algorithm

In order to solve the SOP, we use the speed optimization algorithm (SOA) which was first proposed by Norstad et al. (2011) and Hvattum et al. (2013) for maritime transportation. The algorithm was first adapted by Demir et al. (2012) for ground transportation. The authors stated that the algorithm finds the optimal solution due to convexity of the objective function (Hvattum et al., 2013). We adapt the algorithm proposed by Demir et al. (2012) to our problem. The pseudo-code of the algorithm is presented in Appendix A. The main difference of our algorithm compared to the one proposed by Hvattum et al. (2013) is while calculating the vehicle speeds we consider the time windows, the minimum and maximum speed limits and the optimal speed (v^*).

Kramer et al. (2015) developed a speed and departure time optimization algorithm, which is very similar to the algorithm proposed by Demir et al. (2012). They reformulated the speed optimization problem and proved the optimality of their algorithm by using the necessary and sufficient Karush-Kuhn-Tucker optimality conditions of the reformulated version of the speed optimization problem. Their proof can easily be adapted to prove our version of the speed optimization algorithm.

We note here that the proposed algorithm gives the exact value of vehicle speed that minimizes the fuel consumption, rather than a discretized speed level as in the green location routing problem formulation. Therefore, it provides a more accurate estimation for fuel consumption.

3.2 Iterated Local Search Algorithm

We also develop an Iterated Local Search (ILS) algorithm for the problem. The ILS approach was first proposed by Lourenço et al. (2003). The ILS algorithm has already been applied to several vehicle routing problems along with some location-routing problems in the literature (Derbel et al., 2012; Nguyen et al., 2012).

The main structure of the proposed algorithm is shown in Algorithm 1.

Algorithm 1 Iterated Local Search

```

1:  $Iter \leftarrow 1, f(s^*) \leftarrow \infty$ 
2: for  $Iter \leftarrow 1$  to  $MaxIter$  do
3:   Generate an initial solution  $s$ 
4:    $\bar{s} \leftarrow s, Iter_{NI} \leftarrow 0$ 
5:   while  $Iter_{NI} < MaxIter_{NI}$  do
6:      $s' \leftarrow Local\ Search(s)$ 
7:     if  $f(s') < f(\bar{s})$  then
8:        $\bar{s} \leftarrow s'$ 
9:        $Iter_{NI} \leftarrow 0$ 
10:    end if
11:     $s \leftarrow Perturbation(\bar{s})$ 
12:     $Iter_{NI} \leftarrow Iter_{NI} + 1$ 
13:  end while
14:  if  $f(\bar{s}) < f(s^*)$  then
15:     $s^* \leftarrow \bar{s}$ 
16:  end if
17: end for
18: return  $s^*$  and  $f(s^*)$ 

```

The proposed ILS algorithm consists of three main components; initial solution, local search and perturbation. At each iteration $Iter$, the algorithm first generates an initial feasible solution s , which is also assigned as the incumbent solution \bar{s} (lines 3 to 4). Then, a local search procedure is applied to this initial solution to find a new solution s' (line 6). If the objective function value of this new solution $f(s')$ is less than that of the incumbent solution $f(\bar{s})$, then this new solution s' becomes the incumbent solution \bar{s} (lines 7 to 8). To escape from a local optimum solution, the algorithm perturbs the incumbent solution \bar{s} and generates a new starting solution s (line 11). These local search and perturbation procedures repeat until a certain number $MaxIter_{NI}$ of iterations without improvement is reached (lines 5 to 13). Finally, if the objective function of the incumbent solution $f(\bar{s})$ is less than the that of the global best solution $f(s^*)$, then the incumbent solution \bar{s} replaces the global best solution s^* (lines 14 to 15). The algorithm continues until a certain number $MaxIter$ of iterations is reached (lines 2 to 17).

3.2.1 Initial Solution

Initial feasible solutions to the GLRP are generated by first locating the depots and then assigning the customers to the located depots. The depot decisions are made in two different ways. In the first iteration of the algorithm ($Iter = 1$), we select the first p depots that have the lowest average distances to the customers. In the subsequent iterations ($Iter > 1$), we identify a larger set of $p + k$ candidate depot locations that have the lowest average distances to the customers, where $k > 1$ is an integer, and randomly locate p depots from within this set. Once the depot locations are fixed, customers are assigned to their

nearest depots in the first $\delta\%$ of the total number *MaxIter* of iterations of the algorithm. In the rest of the algorithm, the assignments of customers to depots are done randomly. The effect of such random assignments on the algorithm's performance is numerically investigated in later sections.

To construct the routes, we use the savings algorithm (Clarke and Wright, 1964). At the beginning of the algorithm, vehicles serve only one customer, which means after visiting a customer, the vehicle returns the depot directly without visiting any other customers. After constructing the tours in this manner, the algorithm calculates the potential savings to be gained if two different tours are combined. Then, starting from the maximum savings combination, the algorithm combines tours until there is no savings combinations left. While combining the tours, our version of this algorithm also respects vehicle capacity and customer time window constraints. After constructing the tours, the SOA is applied to find the optimal vehicle speeds.

3.2.2 Local Search

For the local search procedure, initially, the algorithm uses removal and insertion operations between the tours. Initially, two tours are selected; one from which a customer will be removed and the other to which the removed customer will be inserted. The selection of tours are random except for single-customer tours. In this case, a customer from the tour with the highest number of customers is removed and inserted into single-customer tour.

The selection of the customer that will be removed and the selection of the position into which that customer will be inserted are decided as follows. First, the cost of a customer is calculated as the difference of total distance of the tour with and without that customer. The customer with the highest cost on tour is selected to be removed from the former tour. Then, the position that removed customer will be inserted is selected based on its impact on the latter tour. The algorithm selects the position with the lowest impact on the tour in terms of distance and then it inserts the removed customer into that position.

After the removal and insertion operators, the well-known two-opt algorithm proposed by Croes (1958) is used where two edges from a tour are removed and then two resulting paths are reconnected in a different way. In our algorithm, for each tour in the solution, all possible two-opt moves are applied. After these moves, if an improvement is achieved, the same two-opt procedure is applied to the new improved solution until there is no improvement in the solution. Any two-opt move that violates the time window constraints are not allowed in this algorithm. After each two-opt move, the SOA is also applied to the tours to find the optimal vehicle speeds.

3.2.3 Perturbation Search

In the perturbation stage, the algorithm again uses removal and insertion operations between the tours. The tour selection is the same as the one in local search. However, the selection of the customer that will be removed and the selection of the position into which that customer will be inserted are made randomly. Any move that cause an infeasible solution due to the capacity or time window constraints are not allowed in the algorithm.

4 Computational Results

In this section, we present extensive computational results and analyses on the GLRP and also the performance of the solution approaches. The aim of the computational analysis is three-fold. First, we test the formulation proposed for the GLRP and the effect of the valid inequalities on its performance. Second, we conduct a detailed analysis on the GLRP by numerically assessing the effect of a number of parameters, such as depot cost, fuel consumption and emission cost, time windows and depot locations. Third, we compare three solution approaches for the GLRP, namely to use the GLRP formulation and two heuristic methods.

The computational experiments were carried out on a server using 4 AMD Opteron Interlagos 6282 SE and with 96 GB of RAM. All mathematical models and algorithms were implemented in Java. The IBM ILOG CPLEX Optimization Studio version 12.6.1.0 was used as the solver. The time limit was set as two hours for any instance.

4.1 Description of the data set

The instances tested here are from the PRP Library of Demir et al. (2012). The data set in this library consists of randomly selected cities of the United Kingdom with real road distances, but where demands, time windows and service time are randomly generated. The instances are available at <http://apollo.management.soton.ac.uk/prplib.htm>. As the library does not include any information on the cost of a depot, the fixed operating cost of a depot is modeled to be proportional to the distance to the customers. To determine this value, for each depot, the average of the distances from other demand nodes to that depot is calculated, bearing in mind that any demand node can be a depot. Here, we assume that being closer to customers means a more centrally located depot, which can reduce the operational cost of a depot.

The set of speeds are defined from 55 km/h to 90 km/h in 5 km/h increments, resulting in $R =$

{55, 60, 65, 70, 75, 80, 85, 90}. We do not consider any speed level less than 55 km/h based on the results of Demir et al. (2014a) who showed that the optimal vehicle speed to minimize the amount of emission is around 55 km/h for given specific parameter values, irrespective of the vehicle being empty or loaded, and when there are no time related constraints. This assumption is justified by the fact that the vehicles can wait at nodes before the service starts. Therefore, any solution using speed values less than 55 km/h would be dominated.

All other values used for the emission model parameters used can be found in Appendix B (Demir et al., 2012, 2014a).

4.2 Performance of the valid inequalities

This section reports the results of detailed experiments on the performance of the proposed valid inequalities. We use the first four of the 20-node instances from the PRP Library with three different (m, p) pairs as $(3, 1)$, $(3, 2)$, $(3, 3)$, resulting in a total of 12 instances tested here.

The valid inequalities are used in combination to find the best configuration. We do not consider any combinations that include (VI 1.1) and (VI 1.2) together, as they both are subtour breaking constraints. A total of 24 combinations are tested, where each combination is appended to the formulation and solved with CPLEX. We normalize the CPU times against the base case, shown in the first row of the table, in which no valid inequalities are used.

The average results over the 12 instances are presented in Table 3, where the columns titled “Comb.” show the various combinations of the valid inequalities 1.1, 1.2, 2, 3 and 4. In this table, we present only the average values; the average solution time under column “Av. CPU” as well as the average normalized solution time under column “Av. N. CPU”. Detailed results are given in Appendix C.

Table 3: Performance of the valid inequalities

Comb.	Av. CPU	Av. N. CPU	Comb.	Av. CPU	Av. N. CPU	Comb.	Av. CPU	Av. N. CPU
Base	1763.42	1.00	1.1-4	2489.45	2.04	1.1-2-4	1795.16	2.00
1.1	2044.12	1.71	1.2-2	1736.87	1.64	1.1-3-4	1077.80	1.01
1.2	1705.05	1.28	1.2-3	782.14	0.61	1.2-2-3	1250.60	1.21
2	2623.29	2.44	1.2-4	2317.37	1.83	1.2-2-4	2639.75	2.43
3	1426.74	0.92	2-3	1753.66	1.68	1.2-3-4	1045.26	0.93
4	2529.33	2.16	2-4	2997.97	2.86	2-3-4	1841.75	1.52
1.1-2	1272.73	1.71	3-4	2138.74	1.76	1.1-2-3-4	1259.45	1.25
1.1-3	920.89	0.78	1.1-2-3	859.12	0.62	1.2-2-3-4	2061.90	2.16

The results in Table 3 indicate that the combinations 1.2-3 and 1.1-2-3 both provide the two lowest average normalized CPU times equal to 0.61 and 0.62, respectively. In terms of the average solution time, however, the combination 1.2-3 with 782.14s performs better than the combination of 1.1-2-3 with

859.12s, for which reason the former combination will be used in the rest of the experiments.

4.3 Analysis of the GLRP Solutions

We conduct a comprehensive analysis on the GLRP, to test the sensitivity of the solutions against changes in the input parameters, such as the number of depots p , the fixed cost c_k and time windows $[l_i, u_i]$. For this purpose, we generate a larger set of problem instances with $|N| = 10, 15, 20$ and $p = 1, 2, 3$, where, for each pair (N, p) , we choose the minimum value $m^* \in \{2, 3, 4\}$ so that the resulting instance is feasible. Four instances for each (N, p, m^*) are generated, resulting in a total of 36 instances altogether. Details of the instances as well as the experiments are given in Appendix D.

We first present a summary of the results for the new instances in Table 4, which presents the average values over four instances for each combination of (N, p) , averages for each N , and averages across all instances in the last row. The columns titled “Total Cost”, “Depot Cost” and “Fuel Consumption” stand for the optimal objective value, the total cost (in pounds), the fixed cost of depot location (in pounds) and the amount of fuel consumed (in L), separately for weight and speed-induced amounts, respectively. In the last three columns, “Average Speed”, “Distance” and “CPU” represent the average vehicle speed (in km/h), the total distance traversed (in km) and finally the CPU time (in s), respectively.

Table 4: Summary of the computational results for the GLRP

$ N $	p	Total Cost (£)	Depot Cost (£)	Fuel Consumption			Avg. Speed (km/h)	Distance (km)	CPU (s)
				Weight (L)	Speed (L)	Total (L)			
10	1	243.52	140.30	28.07	45.66	73.73	56.02	457.19	6.59
10	2	381.67	288.11	25.69	41.14	66.83	56.25	411.39	8.09
10	3	533.43	442.89	24.87	39.81	64.67	56.39	398.04	7.59
10		386.21	290.43	26.21	42.20	68.41	56.22	422.21	7.42
15	1	294.62	152.37	39.09	62.52	101.61	62.42	599.40	809.93
15	2	435.27	302.02	36.76	58.41	95.18	60.50	568.73	405.52
15	3	587.33	468.44	32.71	52.20	84.92	57.23	520.13	331.86
15		439.07	307.61	36.19	57.71	93.90	60.05	562.75	515.77
20	1	288.76	136.86	42.47	66.03	108.50	56.65	659.87	796.17
20	2	419.98	281.17	38.61	60.55	99.15	56.25	605.96	592.01
20	3	560.12	424.66	37.62	59.14	96.76	56.50	591.71	958.23
20		422.95	280.89	39.56	61.91	101.47	56.47	619.18	782.14
Average		416.08	292.98	33.99	53.94	87.93	57.58	534.71	435.11

As it can be seen from the table, as the value of p is increased, the total cost and the total fixed cost of operating depots also increase by £142.33 and £151.08 on average, respectively. In contrast, increasing the value of p reduces the total amount of fuel consumed by 6.25 L on average, and by 2.41 L and 3.84 L for the weight and speed-induced consumption, respectively. Increasing the number of opening depots

reduces the number of customers to be served in the network, leading to less load on the vehicles and the total distance traveled. The average CPU times for 10, 15 and 20 nodes instances are 7.42, 515.77 and 782.14 s, respectively, which shows the expected increase on the CPU time as the instance sizes increase.

4.3.1 The effect of the depot cost

To assess the effect of depot location decisions on fuel consumption and emissions, we use two different types of depot costs. In the first, depot costs are assigned as being inversely proportional to the average distance to other demand nodes. In the second, depot costs are generated randomly. In Table 5, we present the comparison results for 10, 15 and 20 node problem instances.

Table 5: Different depot cost analysis

N	Base (Directly Proportional)			Inversely Proportional			Random		
	Fuel Cons. (L)	A. Speed (km/h)	Distance (km)	Fuel Cons. (L)	A. Speed (km/h)	Distance (km)	Fuel Cons. (L)	A. Speed (km/h)	Distance (km)
10	68.41	56.22	422.21	65.60	57.94	397.72	64.74	57.13	398.99
15	93.90	60.05	562.75	98.06	57.28	595.24	92.44	58.41	556.71
20	101.47	56.47	619.18	109.63	56.06	666.30	102.10	57.54	619.31
Average	87.93	57.58	534.71	91.10	57.09	553.09	86.43	57.70	525.00

The results indicate that using inversely proportional depot costs yields different results in terms of the depot location or vehicle routes than directly proportional depot costs in all 36 problem instances. As for the GLRP with randomly generated depot cost, the solution change in 35 problem instances, suggesting that location decisions do play a crucial role on fuel consumption and emissions.

Based on the average values shown in the last row of Table 5, using inversely proportional depot costs change depot location and vehicle routes for all instances, resulting in a 3.17 L (3.60%) increase in fuel consumption due to a 18.38 km (3.44%) increase in the total distance traveled. Since the cost of the depot located near to the customers is more expensive, an increase in the total distance traveled and in the fuel consumed is expected. In contrast, using randomly generated depot costs provides a 1.50 L (1.71%) reduction in fuel consumption due to a 9.71 km (1.82%) decrease in the total distance traveled. No matter how depot costs are generated, the problem yields very similar results in terms of average vehicle speed.

4.3.2 The effect of the fuel consumption and emission cost

The results shown in the previous section suggest that the cost of fuel consumption and emissions has a marginal effect on the location decisions, as compared to the fixed depot costs. The cost of fuel consumption can be volatile in practice. In this section, we conduct additional experiments to analyze the sensitivity of the resulting solutions on the changes in the unit fuel cost. First, we test minor (up to \pm

5%) and major (up to $\pm 50\%$) changes in the fuel cost. A summary of the results can be found in Table 6, the columns of which show the number of instances (out of 36) in which the solution has changed in terms of depot location and/or vehicle route, average total depot cost, average fuel consumption, average vehicle speed and average total distance traveled.

Table 6: The effect of increase and decrease on the fuel consumption and emission cost

Change	Fuel Cost (£)	# of instances changed	Depot Cost (£)	Fuel Consumption (L)	Speed (km/h)	Distance (km)
-50%	0.7	5	291.51	89.17	57.73	541.62
-10%	1.26	2	292.11	88.59	57.74	538.20
-5%	1.33	0	292.98	87.93	57.58	534.71
0	1.4	0	292.98	87.93	57.58	534.71
5%	1.47	0	292.98	87.93	57.58	534.71
10%	1.54	1	293.24	87.75	57.38	534.71
50%	2.1	3	293.68	87.52	57.31	533.52

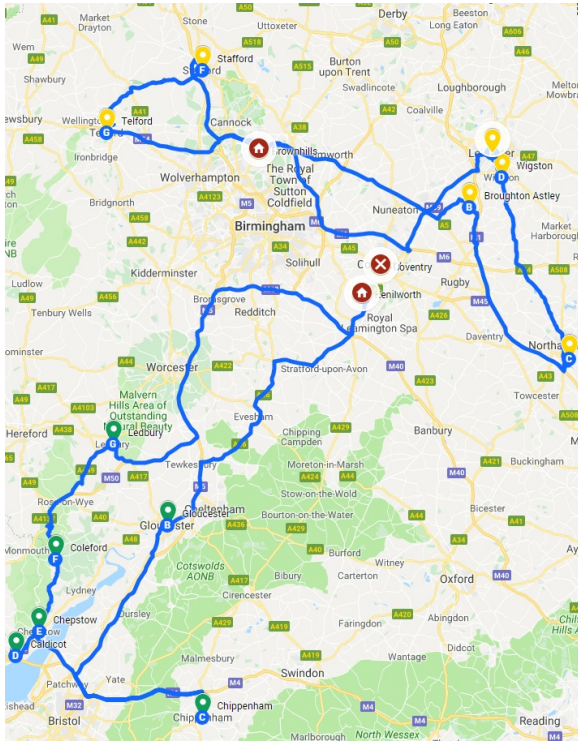
The results in Table 6 indicate that modest and realistic changes of about 5% in the unit fuel consumption and emission cost do not significantly alter the solutions obtained. More extreme variations, however, may result in more observable differences in the solutions obtained. Figures 1(a) and 1(b) serve to illustrate this point, and show two solutions for an instance with 15 nodes, three potential depots and up to two vehicles, with a 50% decrease and increase, respectively, on the unit fuel and emission cost. In both figures, the opened depots which are actively used to serve other customers are represented by houses and the ones do not serve any other customers (except itself) are represented by X marks.

The solution shown in Figures 1(a) uses 107.05 L of fuel, traverses a total distance of 656.53 km and with an average speed equal to 56.43 km/h. The same statistics for the solution shown in Figures 1(b) are 86.35 L, 529.95 km and 55 km/h, respectively. Whereas the solution in Figure 1(a) has a total cost equal to £673.11 of which fuel and emissions account for 11%, the solution in Figure 1(b) has a total cost equal to £806.58 of which 22% is for fuel and emissions.

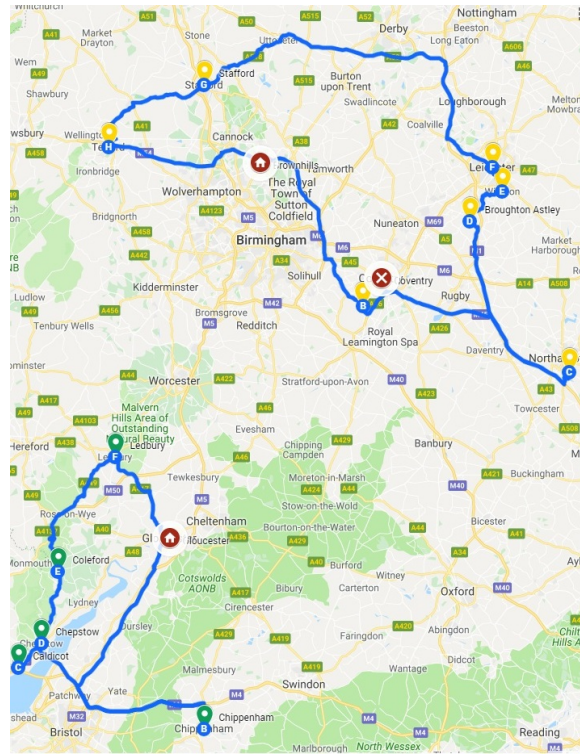
4.3.3 The effect of time windows

The results in Table 4 suggest that speed may have a more significant effect on fuel consumption as compared to that of weight. One of the constraints that affect speed is time windows. To serve customers within the predetermined time windows, in some cases, vehicles have to increase their speed even if it leads to a higher fuel requirements, and consequently emissions. To analyze the effects of time windows on the amount of emissions, we generate new time windows values by narrowing down the original values by 10%, 20%, 30%, 40% and 50%. The results are shown in Table 7.

The average results reported in Table 7 suggest that narrowing down the time windows by up to



(a) Solution obtained with $e = £0.7/L$



(b) Solution obtained with $e = £0.21/L$

Figure 1: Two GLRP solutions on the instance 15.3.2.3 (Google Maps, 2017)

Table 7: Comparisons between the different time windows

	Total Cost (£)	Fixed Cost (£)	Fuel Consumption				
			Weight (L)	Speed (L)	Total (L)	A. Speed (km/h)	Distance (km)
Base	413.00	292.54	32.95	53.09	86.04	56.30	530.45
10%	414.19	292.54	33.10	53.79	86.89	57.16	532.64
20%	415.94	292.34	33.45	54.83	88.29	58.16	540.56
30%	418.86	292.26	33.96	56.22	90.18	57.97	553.70
40%	422.41	292.36	34.72	58.17	92.89	58.71	569.78
50%	429.09	292.87	36.23	61.07	97.30	58.65	610.35

20% does not have a significant impact on the solutions. While the increase on the total cost and the total amount of emission is less than 1% and 3%, respectively, in only two out of 36 instances, the depot locations change. However, for the cases when time windows are narrowed down by more than 30%, there is a significant change on the solutions in terms of vehicle routes and depot locations. The increase on the total amount of emission is 7.97% and 13.09%, when the time windows are narrowed further down by 40% and 50%, respectively. In this case, the increase in the total distance traveled, 7.41% and 13.37%, is due to on the increase in the total amount of emissions. While the average vehicle speed increases in general, for some cases, it remains low for tighter time windows as can be seen from Table 7. The main reason for this unexpected situation is that some of the vehicle routes became infeasible when time windows are too tight that forces vehicles use alternative routes traveling at lower speeds. These new routes, however, eventually increase the total amount of distance traveled and consequently the total amount of emissions.

4.3.4 The effect of the depot location decision

In order to evaluate the impact of the depot location decisions, the GLRP is compared with a version of the problem where the depots are fixed a priori and cannot be changed. For this purpose, the instances in the PRP Library with $p = 1$ are used, where the location of the depot is as described therein (Demir et al., 2012). In this case, the number of nodes is increased by one due to one additional node on which the depot is located. The comparison results are given in Table 8. Detailed results are given in Appendix E.

Table 8: Comparison between the GLRP with and without a fixed depot location

N	GLRP							PRP (GLRP with a known depot location)						
			Fuel Consumption							Fuel Consumption				
	Total Cost (£)	Depot Cost (£)	Weight (L)	Speed (L)	Total (L)	A. Speed (km/h)	Distance (km)	Total Cost (£)	Depot Cost (£)	Weight (L)	Speed (L)	Total (L)	A. Speed (km/h)	Distance (km)
11	242.37	134.67	30.06	46.87	76.93	56.46	469.45	256.20	147.37	30.09	47.65	77.74	56.56	477.40
16	290.60	148.07	38.65	63.15	101.80	58.37	616.35	327.67	173.69	42.62	67.37	109.99	57.27	671.78
21	291.68	134.90	44.09	67.89	111.98	56.41	679.78	322.69	157.55	46.32	71.63	117.96	55.82	718.28
Average	274.88	139.21	37.60	59.30	96.91	57.08	588.53	302.19	159.53	39.68	62.22	101.89	56.55	622.49

The results indicate that in 10 out of 12 instances, the two problems provide different results with respect to the depot location and vehicle routes. For 8 out of these 10 instances, the GLRP results in a reduction in fuel consumption by 4.98 L (4.89%), on average (Table 8). The reduction on the amount of weight and speed-induced consumption is 2.08 and 2.92 L, respectively. The average speed for the GLRP is nearly the same as the fixed depot case, but the total travel distance is reduced by 33.96 km (5.46%) and the total cost by 9.04% in the former.

4.4 Performance of the solution algorithms

In this section, we present computational results on the performance of the CLRSOA and the ILS algorithm in terms of solution quality and computational time compared to solving the GLRP formulation.

For this purpose, four 20-node problem instances with $p = 1, 2, 3$ from PRP data set are used.

For the CLRSOA, preliminary analysis indicate that for some problem instances the optimization process of solving a CumLRP formulation takes too much time. In order to reduce the solution times, we stop the optimization process of the CumLRP formulations after a predetermined time limit and use the resulting incumbent solutions in the “solution pool” for the SOA. The time limit for the optimization process of the CumLRP is set as 10 minutes.

The parameters of the ILS algorithm are chosen after a set of preliminary fine-tuning experiments and are set as follows: $MaxIter = 25$, $MaxIter_{NI} = 50$, $k = 2$ and $\delta = 40$. Since the ILS algorithm contains some random aspects, instances are run five times and the best, average and worst results are reported.

4.4.1 Computational Experiments

This section presents the results obtained by solving the GLRP formulation and two heuristic algorithms for small sized instances and provides a comparison between the solutions and computational time of the aforementioned solution methods with the results of the GLRP formulation which solves 20-node GLRP instances to optimality. We present the comparison results separately for each of the two heuristic algorithms.

The results obtained with the two variants of the CLRSOA are given in Tables 9 & 10, one using the CumLRP and the other using the CumLRP' formulation, respectively. The first three columns show the problem parameters; the number of nodes ($|N|$), instance number (I) and the number (p) of depots to be located, respectively. The columns titled “Obj. Func.” and “S. Time” represent the objective function value (in £) and the solution time (in s) of the corresponding strategy; namely, Dynamic Search (DS), Branch & Bound (BB) and Cut & Branch (CB), respectively. We also report the gap (in %) calculated as $(z^{GLRP} - z^{CLRSOA}) \times 100 / z^{GLRP}$, where z^{GLRP} and z^{CLRSOA} are the objective function values of the GLRP formulation and the CLRSOA, respectively. As all 20-node problem instances are solved to optimality with the GLRP formulation, the gaps correspond to the deviations from the optimal values.

In Tables 9 & 10, some negative gaps are observed. This is due to the SOP being solved exactly within the CLRSOA but with discretized values in the GLRP formulation. The results on Tables 9 & 10 show that all versions of the CLRSOA provide optimal or near optimal solutions in similar amounts of

Table 9: Results of the CLRSOA with the CumLRP formulation for 20-node instances

N	I	p	GLRP Formulation		DS			BB			CB		
			Obj Func. (£)	S. Time (s)	Obj Func. (£)	S. Time (s)	Gap (%)	Obj Func. (£)	S. Time (s)	Gap (%)	Obj Func. (£)	S. Time (s)	Gap (%)
20	1	1	346.34	2864.73	348.46	70.28	0.61	348.46	82.84	0.61	348.46	90.65	0.61
20	1	2	506.47	746.82	512.88	94.19	1.26	512.99	113.72	1.29	512.99	127.25	1.29
20	1	3	673.49	904.23	675.60	59.47	0.31	675.60	105.74	0.31	675.53	53.78	0.30
20	2	1	306.33	67.51	306.30	16.45	-0.01	306.30	16.90	-0.01	306.30	13.96	-0.01
20	2	2	446.75	114.01	446.72	14.06	-0.01	446.72	17.45	-0.01	446.72	25.89	-0.01
20	2	3	600.98	147.81	600.95	16.20	0.00	600.95	22.64	0.00	600.95	39.68	0.00
20	3	1	206.05	100.60	206.04	23.20	-0.01	206.04	37.00	-0.01	206.04	36.24	-0.01
20	3	2	309.15	657.89	309.82	78.70	0.22	309.82	106.65	0.22	309.82	72.98	0.22
20	3	3	412.67	642.50	412.63	69.95	-0.01	412.66	59.38	0.00	413.37	59.30	0.17
20	4	1	296.31	151.82	296.31	61.22	0.00	296.31	45.07	0.00	296.31	44.31	0.00
20	4	2	413.80	189.00	414.36	16.87	0.14	415.78	32.99	0.48	413.81	40.03	0.00
20	4	3	546.22	120.29	546.23	14.04	0.00	546.23	25.32	0.00	546.84	33.57	0.11
Average				558.93		44.55	0.21		55.48	0.24		53.14	0.22

Table 10: Results of the CLRSOA with the CumLRP' formulation for 20-node instances

N	I	p	GLRP Formulation		DS			BB			CB		
			Obj Func. (£)	S. Time (s)	Obj Func. (£)	S. Time (s)	Gap (%)	Obj Func. (£)	S. Time (s)	Gap (%)	Obj Func. (£)	S. Time (s)	Gap (%)
20	1	1	346.34	2864.73	356.09	601.03	2.81	346.48	111.70	0.04	346.57	74.91	0.07
20	1	2	506.47	746.82	506.37	326.74	-0.02	506.37	204.16	-0.02	506.37	130.41	-0.02
20	1	3	673.49	904.23	673.81	163.58	0.05	682.69	252.93	1.36	673.41	80.07	-0.01
20	2	1	306.33	67.51	306.30	19.92	-0.01	306.30	33.21	-0.01	306.30	33.70	-0.01
20	2	2	446.75	114.01	446.72	72.89	-0.01	446.72	63.85	-0.01	446.72	52.94	-0.01
20	2	3	600.98	147.81	601.81	96.13	0.14	601.81	55.51	0.14	600.95	64.03	0.00
20	3	1	206.05	100.60	206.04	75.55	-0.01	206.04	58.66	-0.01	206.04	64.43	-0.01
20	3	2	309.15	657.89	309.11	150.53	-0.01	309.11	153.38	-0.01	309.11	117.05	-0.01
20	3	3	412.67	642.50	412.63	106.51	-0.01	412.63	80.83	-0.01	413.37	127.90	0.17
20	4	1	296.31	151.82	296.31	120.55	0.00	296.31	50.31	0.00	296.31	54.64	0.00
20	4	2	413.80	189.00	413.80	68.43	0.00	413.80	78.24	0.00	413.80	80.47	0.00
20	4	3	546.22	120.29	546.22	31.68	0.00	31.09	159.44	0.00	546.22	63.38	0.00
Average				558.93		152.79	0.24		97.82	0.12		78.66	0.01

time. Among these six versions, CumLRP' formulation with the CB strategy provides the best results. The average gap and the average solution time for CumLRP' with CB version is 0.01% and 78.66 seconds, respectively.

We report the results of the ILS algorithm in Table 11. Each instance is run five times and the table provides the best, average and worst results of these five runs.

Table 11: Results of the ILS algorithm for 20-node instances

			GLRP Formulation		ILS								
					Best			Average			Worst		
$ N $	I	p	Obj. F. (£)	S. Time (s)	Obj. F. (£)	S. Time (s)	Gap (%)	Obj. F. (£)	S. Time (s)	Gap (%)	Obj. F. (£)	S. Time (s)	Gap (%)
20	1	1	346.34	2864.73	346.27	5.15	-0.02	346.27	5.34	-0.02	346.27	5.71	-0.02
20	1	2	506.47	746.82	510.99	6.09	0.89	511.49	6.45	0.99	513.18	6.09	1.32
20	1	3	673.49	904.23	676.59	5.58	0.46	677.93	5.07	0.66	678.27	5.22	0.71
20	2	1	306.33	67.51	308.17	5.91	0.60	308.17	6.23	0.60	308.17	6.38	0.60
20	2	2	446.75	114.01	446.72	8.99	-0.01	451.54	7.76	1.07	460.49	6.81	3.08
20	2	3	600.98	147.81	601.94	6.06	0.16	608.45	6.71	1.24	619.87	5.52	3.14
20	3	1	206.05	100.60	206.04	5.44	-0.01	206.04	5.75	-0.01	206.04	6.20	-0.01
20	3	2	309.15	657.89	309.12	7.65	-0.01	310.61	7.46	0.47	313.67	6.88	1.46
20	3	3	412.67	642.50	415.94	5.54	0.79	418.19	6.19	1.34	421.61	6.54	2.17
20	4	1	296.31	151.82	302.37	5.72	2.05	302.37	6.26	2.05	302.37	6.69	2.05
20	4	2	413.80	189.00	413.80	4.78	0.00	413.80	5.29	0.00	413.80	5.83	0.00
20	4	3	546.22	120.29	546.22	4.59	0.00	546.22	4.85	0.00	546.22	5.13	0.00
Average				558.93		5.96	0.41		6.11	0.70		6.08	1.21

Similar to results of the CLRSOA, since the SOP is solved exactly within the ILS algorithm, negative gaps can be observed in Table 11. Table 11 indicates that the ILS algorithm generally provides very good results in terms of solution quality and computational time. The average optimality gap and the average solution time of the ILS in the best case scenario is 0.41% and 5.96 seconds and 1.21% and 6.08 seconds in the worst case scenario.

In order to explore different solution and escape possible local optimal solution, we increase the effects of randomness on the algorithm. Therefore, we conduct experiments with higher $MaxIter$ and lower δ values. In addition to (25, 40%) combination of $MaxIter$ and δ values for which the results are reported in Table 12, we also report the summary results for the combinations; (50, 20%) and (100, 10%).

Table 12: ($MaxIter, \delta$) analysis for ILS algorithm

Combination	Best		Average		Worst	
	S. Time (s)	Gap (%)	S. Time (s)	Gap (%)	S. Time (s)	Gap (%)
(25, 40%)	5.96	0.41	6.11	0.70	6.08	1.21
(50, 20%)	12.58	0.37	12.71	0.79	12.84	1.19
(100, 10%)	26.75	0.28	27.49	0.50	27.84	0.71

The results on Table 12 indicate that increasing number of iterations results with higher solution times, but better solutions. With 50 iterations, the average optimality gap in the best case scenario is

0.37% and with 100 iterations it becomes 0.28%. On average of five experiments, the average optimality gaps are 0.79% with 50 iterations and 0.50% with 100 iterations. The solution times are approximately 12 and 25 seconds for 50 and 100 iterations, respectively. Since solution times up to 25 seconds can be acceptable, we propose to use the algorithm with the 100-iteration version.

In conclusion, compared to the CLRSOA, the solutions found by the ILS algorithm are not as good as the ones obtained by the CLRSOA, but in terms of solution time the ILS algorithm performs better than the CLRSOA. So, for small sized instances, the CLRSOA is very efficient alternative to solve the GLRP.

4.5 Computational analysis for large sized instances

We also conduct computational analysis on four different 100-node problem instances with three different p values as 5, 7, 10. Due to computational times required, we do not use the CLRSOA to solve large sized problem instances, and only conduct the experiments with the ILS algorithm using the (100, 10%) combination for the $(MaxIter, \delta)$ setting. The results can be found in Table 13.

Table 13: Results of the ILS algorithm for 100-node instances

$ N $	I	p	Total Cost (£)	Depot Cost (£)	Fuel Consumption			Avg. Speed (km/h)	Distance (km)	S. Time (s)
					Weight (L)	Speed (L)	Total (L)			
100	1	5	1407.89	848.78	157.93	241.44	399.36	55.84	2417.27	820.04
100	1	7	1748.75	1184.16	159.43	243.85	403.27	55.85	2441.51	952.13
100	1	10	2234.23	1715.62	147.00	223.44	370.44	56.20	2225.54	1050.34
100	2	5	1395.32	851.00	155.40	233.40	388.80	55.42	2343.09	963.34
100	2	7	1728.97	1191.50	152.48	231.43	383.91	55.20	2324.25	1295.47
100	2	10	2228.81	1714.27	145.90	221.63	367.53	55.19	2225.86	1190.75
100	3	5	1047.81	618.20	121.41	185.45	306.86	55.49	1860.54	1118.73
100	3	7	1288.65	871.05	118.03	180.25	298.29	55.49	1808.33	1003.43
100	3	10	1667.98	1251.96	117.74	179.42	297.16	55.50	1780.32	1122.83
100	4	5	1230.91	715.77	146.85	221.11	367.96	55.19	2220.62	839.01
100	4	7	1510.00	1002.33	143.59	219.03	362.62	55.19	2199.74	1089.31
100	4	10	1917.73	1456.52	129.79	199.65	329.44	55.19	2005.07	1308.53

As it can be seen from Table 13, increasing the value of p leads to an increase in the total cost and the total fixed cost of operating depots. In contrast, as the value of p is increased, the total amount of fuel consumed and the total distance traveled generally reduces. The difference between average vehicle speeds for different p values can be considered as insignificant, suggesting that the vehicle speed remains stable. In addition, increasing the value of p generally increases the required solution time.

5 Conclusions and Managerial Implications

In this study, we have introduced the GLRP as a combination of the traditional LRP and the more recently studied PRP, in which fuel consumption and CO₂ emissions are explicitly considered. We have developed a mixed integer programming formulation for the GLRP, and described a group of preprocessing rules and valid inequalities to strengthen the formulation. Additionally, we have proposed two heuristic algorithms to solve small and larger sized instances in reasonable times. For the computational study of the GLRP, we have conducted different sensitivity analyses by changing some key parameters such as the number of depots to be opened, the fixed cost of operating depots and the fuel consumption and emission cost. Additionally, we also evaluate the impacts of time windows and depot location decision on fuel consumption. Finally, we compare the GLRP formulation and the proposed heuristic approaches in terms of solution quality and time.

The overall results show that including the “green” aspect in the objective function through fuel consumption and emissions does affect the optimal solutions. It is possible to draw a number of managerial insights from the results given in the previous section. First, depot locations must be explicitly considered in combination with the routing decisions for reductions not only in cost, but also in fuel consumption, resulting in lesser environmental impact. In particular, it may seem attractive to locate depots where it is cheaper to do so, but this may have a knock-on effect on the weight and speed-induced fuel consumption, resulting in a more expensive solution overall. Second, any opportunity that will allow to use looser time windows in making deliveries should be explored by operators, given that such constraints are generally seen to increase speed and distance, along with the associated fuel consumption. Finally, the results suggest that it may be beneficial to locate depots to areas for which heavy deliveries are to be regularly made.

Finally, the performance of the heuristic algorithms indicate that while the CLRSOA is a very effective approach to solve the GLRP for small sized instances, the ILS algorithm can be used to solve larger sized instances in reasonable solution times compared to both the GLRP formulation and the CLRSOA.

Acknowledgment

The authors thank anonymous reviewers and the editor for their valuable comments on an earlier version of this paper that resulted in improved content and exposition.

References

- Achuthan, N. R., Caccetta, L. and Hill, S. P. (2003), 'An improved branch-and-cut algorithm for the capacitated vehicle routing problem', *Transportation Science* **37**(2), 153–169.
- Barth, M. and Boriboonsomsin, K. (2008), 'Real-world carbon dioxide impacts of traffic congestion', *Transportation Research Record: Journal of the Transportation Research Board* **2058**(1), 163–171.
- Barth, M., Younglove, T. and Scora, G. (2005), Development of a heavy-duty diesel modal emissions and fuel consumption model, Technical report, California Partners for Advanced Transit and Highways (PATH), Institute of Transportation Studies, University of California at Berkeley.
- Bektaş, T. and Laporte, G. (2011), 'The pollution-routing problem', *Transportation Research Part B: Methodological* **45**(8), 1232–1250.
- Clarke, G. and Wright, J. W. (1964), 'Scheduling of vehicles from a central depot to a number of delivery points', *Operations Research* **12**(4), 568–581.
- Croes, G. A. (1958), 'A method for solving traveling-salesman problems', *Operations Research* **6**(6), 791–812.
- Dantzig, G., Fulkerson, R. and Johnson, S. (1954), 'Solution of a large-scale traveling-salesman problem', *Journal of the Operations Research Society of America* **2**(4), 393–410.
- Dekker, R., Bloemhof, J. and Mallidis, I. (2012), 'Operations research for green logistics—An overview of aspects, issues, contributions and challenges', *European Journal of Operational Research* **219**(3), 671–679.
- Demir, E., Bektaş, T. and Laporte, G. (2012), 'An adaptive large neighborhood search heuristic for the Pollution-Routing Problem', *European Journal of Operational Research* **223**(2), 346–359.
- Demir, E., Bektaş, T. and Laporte, G. (2014a), 'The bi-objective pollution-routing problem', *European Journal of Operational Research* **232**(3), 464–478.
- Demir, E., Bektaş, T. and Laporte, G. (2014b), 'A review of recent research on green road freight transportation', *European Journal of Operational Research* **237**(3), 775–793.
- Derbel, H., Jarboui, B., Hanafi, S. and Chabchoub, H. (2012), 'Genetic algorithm with iterated local search for solving a location-routing problem', *Expert Systems with Applications* **39**(3), 2865–2871.
- DHL (2012), 'DHL bundles competences at a new logistics center in Milan'. Available from: http://www.dhl.com/en/press/releases/releases_2012/logistics/040312.html [Accessed 23 February 2017].
- DHL (2014), 'Self-driving vehicles in logistics'. Available from: http://www.dhl.com/content/dam/downloads/g0/about_us/logistics_insights/dhl_self_driving_vehicles.pdf [Accessed 13 December 2017].
- DHL (2016), 'DHL express expands at Milano Malpensa: new hub in the cargo city'. February 17, 2016. Available from: http://www.seamilano.eu/sites/sea14.message-asp.com/files/downloads/20160217_cs_dhl_sea_def_en.pdf [Accessed 12 December 2017].
- Dougherty, C. (2017), 'Self-driving trucks may be closer than they appear', *The New York Times*. November 13, 2017. Available from: <https://www.nytimes.com/2017/11/13/business/self-driving-trucks.html> [Accessed 20 December 2017].
- Drexler, M. and Schneider, M. (2015), 'A survey of variants and extensions of the location-routing problem', *European Journal of Operational Research* **241**(2), 283–308.
- Eskandarpour, M., Dejax, P., Miemczyk, J. and Péton, O. (2015), 'Sustainable supply chain network design: An optimization-oriented review', *Omega* **54**, 11–32.

- FedEx (2011), 'Inbound logistics recognizes FedEx as top green supply chain partner'. Available from: <http://about.van.fedex.com/newsroom/united-states-english/inbound-logistics-recognizes-fedex-as-top-green-supply-chain-partner/> [Accessed 25 February 2017].
- FedEx (2016), 'FedEx 2016 global citizenship report Deliver it forward'. Available from: http://csr.fedex.com/pdfs/FedEx_2016_Global_Citizenship_Report_Single.pdf [Accessed 14 December 2017].
- Figliozzi, M. A. (2010), 'Vehicle routing problem for emissions minimization', *Transportation Research Record: Journal of the Transportation Research Board* **2197**(1), 1–7.
- Figliozzi, M. A. (2011), 'The impacts of congestion on time-definitive urban freight distribution networks CO₂ emission levels: Results from a case study in Portland, Oregon', *Transportation Research Part C: Emerging Technologies* **19**(5), 766–778.
- Govindan, K., Jafarian, A., Khodaverdi, R. and Devika, K. (2014), 'Two-echelon multiple-vehicle location-routing problem with time windows for optimization of sustainable supply chain network of perishable food', *International Journal of Production Economics* **152**, 9–28.
- Hvattum, L. M., Norstad, I., Fagerholt, K. and Laporte, G. (2013), 'Analysis of an exact algorithm for the vessel speed optimization problem', *Networks* **62**(2), 132–135.
- Jabali, O., Woensel, T. and de Kok, A. (2012), 'Analysis of travel times and CO₂ emissions in time-dependent vehicle routing', *Production and Operations Management* **21**(6), 1060–1074.
- Kara, I., Kara, B. Y. and Yetis, M. K. (2007), Energy minimizing vehicle routing problem, in A. Dress, X. Yinfeng and Z. Binhai, eds, 'Combinatorial Optimization and Applications, Lecture Notes in Computer Science, vol 4616', Springer Berlin Heidelberg, pp. 62–71.
- Karaoglan, I., Altıparmak, F., Kara, I. and Dengiz, B. (2012), 'The location-routing problem with simultaneous pickup and delivery: Formulations and a heuristic approach', *Omega* **40**(4), 465–477.
- Khoei, A. A., Süral, H. and Tural, M. K. (2017), 'Time-dependent green Weber problem', *Computers & Operations Research* **88**, 316–323.
- Koç, Ç., Bektaş, T., Jabali, O. and Laporte, G. (2016), 'The impact of depot location, fleet composition and routing on emissions in city logistics', *Transportation Research Part B: Methodological* **84**, 81–102.
- Kramer, R., Maculan, N., Subramanian, A. and Vidal, T. (2015), 'A speed and departure time optimization algorithm for the pollution-routing problem', *European Journal of Operational Research* **247**(3), 782–787.
- Lin, C., Choy, K. L., Ho, G. T., Chung, S. and Lam, H. (2014), 'Survey of green vehicle routing problem: Past and future trends', *Expert Systems with Applications* **41**(4), 1118–1138.
- Linshi, J. (2015), 'Meet the country's first self-driving semi truck', *Time*. May 6, 2015. Available from: <http://time.com/3848456/self-driving-freightliner-truck/> [Accessed 27 December 2017].
- Lourenço, H. R., Martin, O. C. and Stützle, T. (2003), Iterated local search, in F. W. Glover and G. A. Kochenberger, eds, 'Handbook of metaheuristics', Springer, pp. 320–353.
- Marshall, A. (2017), 'The Us Postal Service is building a self-driving mail truck', *Wired*. October 9, 2017. Available from: <https://www.wired.com/story/postal-service-office-self-driving-mail-trucks/> [Accessed 15 December 2017].
- Miller, C. E., Tucker, A. W. and Zemlin, R. A. (1960), 'Integer programming formulation of traveling salesman problems', *Journal of the Association for Computing Machinery (JACM)* **7**(4), 326–329.

- Mirzapour Al-e hashem, S. and Rezik, Y. (2014), 'Multi-product multi-period inventory routing problem with a transshipment option: A green approach', *International Journal of Production Economics* **157**, 80–88.
- Nguyen, V.-P., Prins, C. and Prodhon, C. (2012), 'A multi-start iterated local search with tabu list and path relinking for the two-echelon location-routing problem', *Engineering Applications of Artificial Intelligence* **25**(1), 56–71.
- Norstad, I., Fagerholt, K. and Laporte, G. (2011), 'Tramp ship routing and scheduling with speed optimization', *Transportation Research Part C: Emerging Technologies* **19**(5), 853–865.
- Oberscheider, M., Zazgornik, J., Henriksen, C. B., Gronalt, M. and Hirsch, P. (2013), 'Minimizing driving times and greenhouse gas emissions in timber transport with a near-exact solution approach', *Scandinavian Journal of Forest Research* **28**(5), 493–506.
- Palmer, A. (2007), The development of an integrated routing and carbon dioxide emissions model for goods vehicles, PhD thesis, Cranfield University.
- Prodhon, C. and Prins, C. (2014), 'A survey of recent research on location-routing problems', *European Journal of Operational Research* **238**(1), 1–17.
- Qian, J. and Eglese, R. (2014), 'Finding least fuel emission paths in a network with time-varying speeds', *Networks* **63**(1), 96–106.
- Salhi, S. and Rand, G. K. (1989), 'The effect of ignoring routes when locating depots', *European Journal of Operational Research* **39**(2), 150–156.
- Sbihi, A. and Eglese, R. W. (2010), 'Combinatorial optimization and green logistics', *Annals of Operations Research* **175**(1), 159–175.
- Scora, G. and Barth, M. (2006), Comprehensive modal emissions model, version 3.01 User's guide, Technical report, Centre for Environmental Research and Technology. University of California, Riverside, United States of America.
- Singh, R. R. and Gaur, D. R. (2017), Cumulative VRP: A simplified model of green vehicle routing, in D. Cinar, K. Gakis and P. M. Pardalos, eds, 'Sustainable Logistics and Transportation: Optimization Models and Algorithms', Springer Cham, pp. 39–55.
- Stevens, L. and Higgins, T. (2017), 'Amazon forms team to focus on driverless technology', *The Wall Street Journal*. April 24, 2017. Available from: <https://www.wsj.com/articles/amazon-team-focuses-on-exploiting-driverless-technology-1493035203> [Accessed 27 December 2017].
- Toro, E. M., Franco, J. F., Echeverri, M. G. and Guimarães, F. G. (2017), 'A multi-objective model for the green capacitated location-routing problem considering environmental impact', *Computers & Industrial Engineering* **110**, 114–125.
- Tricoire, F. and Parragh, S. N. (2017), 'Investing in logistics facilities today to reduce routing emissions tomorrow', *Transportation Research Part B: Methodological* **103**, 56–67.
- Ubeda, S., Arcelus, F. and Faulin, J. (2011), 'Green logistics at Eroski: A case study', *International Journal of Production Economics* **131**(1), 44–51.
- Unilever (2017), 'Going to market - reducing transport emissions'. Available from: <https://www.unilever.com/sustainable-living/the-sustainable-living-plan/reducing-environmental-impact/greenhouse-gases/going-to-market-reducing-transport-emissions/> [Accessed 9 March 2017].

- UPS (2015), Corporate sustainability report, Technical report. Available from: https://sustainability.ups.com/media/ups-pdf-interactive/UPS_2015_CSR.pdf [Accessed 9 March 2017].
- Varsei, M. and Polyakovskiy, S. (2017), 'Sustainable supply chain network design: A case of the wine industry in Australia', *Omega* **66**, 236–247.
- Volvo (2012), 'SARTRE road train premiere on public roads'. May 28, 2012. Available from: <https://www.media.volvocars.com/global/en-gb/media/pressreleases/43899> [Accessed 27 December 2017].
- Ward, M. (2011), 'Road train technology trials get rolling', *BBC* . January 18, 2011. Available from: <http://www.bbc.com/news/technology-12215915> [Accessed 27 December 2017].
- Woyke, E. (2017), 'FedEx bets on automation as it prepares to fend off Uber and Amazon', *MIT Technology Review* . February 3, 2017. Available from: <https://www.technologyreview.com/s/602896/fedex-bets-on-automation-as-it-prepares-to-fend-off-uber-and-amazon/> [Accessed 27 December 2017].
- Wysocky, K. (2014), 'Mercedes' self-driving truck', *BBC* . November 13, 2014. Available from: <http://www.bbc.com/autos/story/20140926-mercedes-self-driving-truck> [Accessed 27 December 2017].

Appendices

Appendix A: Speed Optimization Algorithm

The decision variables to be optimized in the algorithm are as follows: the vehicle speed between node $i \in N$ and $i + 1 \in N$ is denoted by v_i . e_i and \bar{e}_i represent the arrival and departure time from node $i \in N$.

Algorithm 2 Speed Optimization Algorithm (SOA)

initialize: $s \leftarrow 0, e \leftarrow n, violation \leftarrow 0, p \leftarrow 0, k \leftarrow 1, e_0 = \bar{e}_0 = l_0 = u_0 = 0, D = \sum_{i=s}^{e-1} d_i, S = \sum_{i=s}^e s_i$

```
1: for  $i = s + 1$  to  $e$  do
2:    $v_{i-1} \leftarrow D / (u_e + t_e - \max\{l_s, e_s\} - S)$ 
3:   if  $k \neq 1$  then
4:     if  $\bar{e}_{i-1} + d_{i-1}/v_{i-1} < l_i$  and  $\bar{e}_i \geq l_i + s_i$  then
5:        $v_{i-1} \leftarrow d_{i-1} / (l_i - \bar{e}_{i-1})$ 
6:     else if  $\bar{e}_{i-1} + d_{i-1}/v_{i-1} < u_i$  and  $\bar{e}_i \geq u_i + s_i$  then
7:        $v_{i-1} \leftarrow d_{i-1} / (u_i - \bar{e}_{i-1})$ 
8:     end if
9:   end if
10:   $v_{i-1}^* \leftarrow OptimalSpeed$ 
11:  if  $v_{i-1} < v^l$  then
12:     $v_{i-1} \leftarrow v^l$ 
13:  else if  $v_{i-1} > v^u$  then
14:     $v_{i-1} \leftarrow v^u$ 
15:  end if
16:  if  $v_{i-1}^* > v_{i-1}$  then
17:     $v_{i-1} \leftarrow v_{i-1}^*$ 
18:  end if
19:  if  $k = 1$  then
20:     $e_i = \bar{e}_{i-1} + d_{i-1}/v_{i-1}$ 
21:     $\bar{e}_i = e_i + s_i$ 
22:  else if  $k \neq 1$  then
23:    if  $i \neq e$  then
24:       $e_i = \bar{e}_{i-1} + d_{i-1}/v_{i-1}$ 
25:       $\bar{e}_i = e_i + s_i$ 
26:    end if
27:  end if
28:   $g_i \leftarrow \max\{0, e_i - u_i, l_i + s_i - \bar{e}_i\}$ 
29:  if  $g_i > violation$  then
30:     $violation \leftarrow g_i$ 
31:     $p \leftarrow i$ 
32:  end if
33: end for
34:  $k \leftarrow k + 1$ 
35: if  $violation > 0$  and  $e_p > u_p$  then
36:    $\bar{e}_p \leftarrow u_p + s_p$ 
37:   Speed Optimization Algorithm( $s, p$ )
38:   Speed Optimization Algorithm( $p, e$ )
39: end if
40: if  $violation > 0$  and  $\bar{e}_p < l_p + s_p$  then
41:    $\bar{e}_p \leftarrow l_p + s_p$ 
42:   Speed Optimization Algorithm( $s, p$ )
43:   Speed Optimization Algorithm( $p, e$ )
44: end if
```

Appendix B: Parameter Values for CMEM

Notation	Description	Typical Values
e	Emission and fuel consumption cost (£/L)	1.4
w	Curb weight (kg)	6350
k	Engine friction factor (kJ/rev/L)	0.2
Υ	Engine speed (rev/s)	33
V	Engine displacement (L)	5
a	Acceleration (m/s ²)	0
g	Gravitational constant (m/s ²)	9.81
θ	Road Angle	0
C_r	Coefficient of rolling resistance	0.01
C_d	Coefficient of aerodynamic drag	0.7
ρ	Air density (kg/m ³)	1.2041
S	Frontal Surface Area (m ²)	3.912
n_{tf}	Vehicle drive train efficiency	0.4
η	Efficiency parameter for diesel engines	0.9
ξ	Fuel to air mass ratio	1
κ	Heating value of a typical diesel fuel (kJ/g)	44
ψ	Conversion factor of fuel (g/s) to (L/s)	737
P_{acc}	Engine power demand	0

Appendix C: Performance of the valid inequalities

Comb.	20.1.3.1		20.1.3.2		20.1.3.3		20.2.3.1		20.2.3.2		20.2.3.3		20.3.3.1		20.3.3.2		20.3.3.3		20.4.3.1		20.4.3.2		20.4.3.3		Av. N. CPU
	CPU	N. CPU	CPU	N. CPU	CPU	N. CPU	CPU	N. CPU	CPU	N. CPU	CPU	N. CPU	CPU	N. CPU	CPU	N. CPU	CPU	N. CPU	CPU	N. CPU	CPU	N. CPU	CPU	N. CPU	
Base	3483.90	1.00	6233.13	1.00	900.50	1.00	158.88	1.00	219.44	1.00	617.66	1.00	529.51	1.00	653.21	1.00	639.41	1.00	190.46	1.00	953.75	1.00	6581.21	1.00	1.00
1.1	7200.00	2.07	2275.56	0.37	1948.22	2.16	148.63	0.94	148.05	0.67	714.99	1.16	410.59	0.78	1038.59	1.59	745.07	1.17	788.38	4.14	4637.97	4.86	4473.36	0.68	1.71
1.2	1324.21	0.38	6274.56	1.01	890.35	0.99	103.69	0.65	292.39	1.33	310.64	0.50	476.95	0.90	892.33	1.37	823.77	1.29	182.92	0.96	5149.58	5.40	3739.19	0.57	1.28
2	5037.88	1.45	2048.76	0.33	1448.65	1.61	113.06	0.71	204.39	0.93	589.01	0.95	438.25	0.83	4874.25	7.46	3755.76	5.87	460.43	2.42	5309.04	5.57	7200.00	1.09	2.44
3	5556.02	1.59	1058.99	0.17	675.16	0.75	75.42	0.47	96.34	0.44	364.03	0.59	145.68	0.28	598.22	0.92	534.12	0.84	146.91	0.77	3437.06	3.60	4432.87	0.67	0.92
4	2452.66	0.70	6921.07	1.11	1812.97	2.01	288.08	1.81	490.54	2.24	1416.93	2.29	672.08	1.27	1532.30	2.35	1614.65	2.53	231.59	1.22	7200.00	7.55	5719.12	0.87	2.16
1.1-2	649.98	0.19	1346.65	0.22	1365.05	1.52	114.70	0.72	188.30	0.86	255.94	0.41	308.34	0.58	2884.72	4.42	914.06	1.43	1277.57	6.71	2892.55	3.03	3074.87	0.47	1.71
1.1-3	4313.98	1.24	1062.72	0.17	1203.24	1.34	73.55	0.46	215.01	0.98	196.90	0.32	420.47	0.79	795.37	1.22	812.68	1.27	118.39	0.62	780.73	0.82	1057.67	0.16	0.78
1.1-4	7200.00	2.07	2248.76	0.36	2310.59	2.57	218.22	1.37	253.28	1.15	576.12	0.93	683.57	1.29	1938.31	2.97	2117.82	3.31	244.14	1.28	5905.83	6.19	6176.75	0.94	2.04
1.2-2	1277.91	0.37	3091.40	0.50	831.54	0.92	101.11	0.64	160.09	0.73	421.55	0.68	355.25	0.67	5503.84	8.43	914.34	1.43	116.16	0.61	3889.35	4.08	4179.90	0.64	1.64
1.2-3	2864.73	0.82	746.82	0.12	904.23	1.00	67.51	0.42	114.01	0.52	147.81	0.24	100.60	0.19	657.89	1.01	642.50	1.00	151.82	0.80	849.33	0.89	2138.37	0.32	0.61
1.2-4	2624.10	0.75	7200.00	1.16	1403.27	1.56	157.05	0.99	295.42	1.35	434.63	0.70	712.14	1.34	1855.65	2.84	1705.02	2.67	225.44	1.18	6318.59	6.62	4877.18	0.74	1.83
2-3	3037.83	0.87	1268.50	0.20	807.22	0.90	98.65	0.62	98.24	0.45	192.62	0.31	335.38	0.63	934.32	1.43	5519.49	8.63	122.92	0.65	4688.20	4.92	3940.58	0.60	1.68
2-4	5675.14	1.63	1866.87	0.30	2290.42	2.54	216.32	1.36	269.70	1.23	926.11	1.50	641.49	1.21	2256.36	3.45	7200.00	11.26	233.27	1.22	5711.39	7.55	7200.00	1.09	2.86
3-4	4245.84	1.22	2245.85	0.36	1598.37	1.77	143.60	0.90	193.31	0.88	283.05	0.46	1033.87	1.95	1942.19	2.97	1585.92	2.48	228.02	1.20	5711.39	5.99	6453.51	0.98	1.76
1.1-2-3	3648.49	1.05	1138.23	0.18	692.01	0.77	65.14	0.41	78.21	0.36	220.88	0.36	154.47	0.29	769.89	1.18	760.86	1.19	115.09	0.60	686.94	0.72	1979.28	0.30	0.62
1.1-2-4	1571.87	0.45	3041.08	0.49	2401.91	2.67	221.09	1.39	235.59	1.07	485.53	0.79	563.95	1.07	1992.42	3.05	5046.06	7.89	615.66	3.23	1217.68	1.28	4149.09	0.63	2.00
1.1-3-4	2504.64	0.72	1868.04	0.30	1403.78	1.56	107.07	0.67	149.81	0.68	154.19	0.25	290.32	0.55	1297.45	1.99	1160.73	1.82	261.01	1.37	1875.35	1.97	1861.18	0.28	1.01
1.2-2-3	680.57	0.20	1262.73	0.20	906.13	1.01	61.90	0.39	80.55	0.37	80.55	0.13	92.59	0.17	3998.63	6.12	552.02	0.86	107.41	0.56	3869.96	4.06	3314.18	0.50	1.21
1.2-2-4	2594.95	0.74	6093.46	0.98	1558.58	1.73	218.15	1.37	294.14	1.34	379.93	0.62	405.38	0.77	7200.00	11.02	2249.01	3.52	152.83	0.80	5168.52	5.42	5362.01	0.81	2.43
1.2-3-4	1034.52	0.30	1718.78	0.28	1120.11	1.24	107.14	0.67	97.33	0.44	206.15	0.33	210.25	0.40	1833.63	2.81	1436.42	2.25	148.31	0.78	1098.12	1.15	3532.37	0.54	0.93
2-3-4	1647.79	0.47	1634.40	0.26	1939.98	2.15	132.87	0.84	140.27	0.64	422.97	0.68	213.83	0.40	1909.03	2.92	1682.95	2.63	163.84	0.86	5013.03	5.26	7200.00	1.09	1.52
1.1-2-3-4	4163.60	1.20	1311.91	0.21	2832.83	3.15	121.69	0.77	104.47	0.48	221.60	0.36	510.64	0.96	2582.24	3.95	1140.17	1.78	199.32	1.05	894.07	0.94	1030.88	0.16	1.25
1.2-2-3-4	4798.35	1.38	1604.25	0.26	1390.62	1.54	133.27	0.84	149.26	0.68	246.74	0.40	156.11	0.29	5112.90	7.83	5492.51	8.59	136.18	0.72	2802.33	2.94	2720.23	0.41	2.16

Appendix D: GLRP results for 10, 15 and 20-node instances

N	I	m	p	Fuel Consumption								# of Vehicles	Average Speed (km/h)	Distance (km)	CPU (s)
				Total Cost (£)	Depot Cost (£)	Weight (L)	Speed (L)	Total (L)	Weight (L)	Speed (L)	Total (L)				
10	1	2	1	197.58	114.14	23.00	36.60	59.60	2	55.00	367550	4.59			
10	1	2	2	303.55	232.10	19.42	31.62	51.03	2	55.00	317520	2.15			
10	1	2	3	433.75	366.09	18.13	30.20	48.33	2	55.00	303250	7.02			
10	2	2	1	265.07	146.78	31.32	53.18	84.50	2	59.09	528590	7.87			
10	2	2	2	419.10	308.31	29.73	49.40	79.13	2	55.00	496161	11.83			
10	2	2	3	578.19	471.84	29.10	46.86	75.96	2	55.00	470610	11.80			
10	3	2	1	267.16	158.64	30.30	47.21	77.51	2	55.00	474160	10.61			
10	3	2	2	410.68	318.20	25.64	40.42	66.05	2	55.00	405910	8.57			
10	3	2	3	574.54	484.79	24.53	39.57	64.10	2	55.00	397400	3.70			
10	4	2	1	244.29	141.64	27.67	45.65	73.32	2	55.00	458440	3.27			
10	4	2	2	393.37	293.84	27.98	43.11	71.10	2	60.00	425974	9.82			
10	4	2	3	547.25	448.82	27.69	42.61	70.30	2	60.56	420904	7.85			
15	1	2	1	310.23	158.81	42.04	66.12	108.16	2	64.06	615352	1333.66			
15	1	2	2	462.84	313.80	41.26	65.19	106.46	2	64.67	606032	70.87			
15	1	2	3	616.77	478.11	38.89	60.15	99.04	2	57.50	599362	39.63			
15	2	2	1	241.04	128.25	30.85	49.71	80.57	2	60.00	487951	28.19			
15	2	2	2	366.93	260.82	29.18	46.61	75.79	2	56.67	466791	16.36			
15	2	2	3	497.23	396.15	27.38	44.82	72.20	2	56.79	448811	29.37			
15	3	2	1	360.18	194.25	46.40	72.13	118.53	2	61.88	712440	1450.34			
15	3	2	2	544.97	384.44	44.82	69.85	114.67	2	61.33	690470	1517.44			
15	3	2	3	746.14	625.25	33.58	52.77	86.35	2	55.00	529950	1238.87			
15	4	2	1	267.04	128.16	37.09	62.11	99.20	2	63.75	581850	427.52			
15	4	2	2	366.35	249.03	31.79	52.00	83.80	2	59.33	511640	17.40			
15	4	2	3	489.17	374.26	31.00	51.08	82.08	2	59.64	502380	19.58			
20	1	3	1	346.34	168.82	49.94	76.87	126.81	3	57.95	763601	2864.73			
20	1	3	2	506.47	353.12	43.06	66.47	109.53	3	57.62	661061	746.82			
20	1	3	3	673.49	522.26	42.38	65.65	108.03	3	58.00	652861	904.23			
20	2	3	1	306.33	145.12	44.47	70.68	115.15	3	55.23	709652	67.51			
20	2	3	2	446.75	291.04	42.74	68.48	111.22	3	55.24	687622	114.01			
20	2	3	3	600.98	450.16	41.20	66.53	107.73	3	55.25	667991	147.81			
20	3	3	1	206.05	101.97	29.18	45.17	74.34	3	58.41	449111	100.60			
20	3	3	2	309.15	210.79	27.43	42.82	70.25	3	57.14	428331	657.89			
20	3	3	3	412.67	316.58	26.95	41.69	68.64	3	57.75	416151	642.5			
20	4	3	1	296.31	131.54	46.29	71.40	117.70	3	55.00	717110	151.82			
20	4	3	2	417.54	269.71	41.19	64.41	105.59	3	55.00	646830	849.33			
20	4	3	3	553.35	409.63	39.94	62.71	102.66	3	55.00	629820	2138.37			

Appendix E: The impact of the location decision

N	I	m	p	GLRP								GLRP with a known depot location							
				Fuel Consumption				Avg. Speed				Fuel Consumption				Avg. Speed			
				Total Cost (£)	Depot Cost (£)	Weight (L)	Speed (L)	Total (L)	Avg. Speed (km/h)	Distance (km)	Total Cost (£)	Depot Cost (£)	Weight (L)	Speed (L)	Total (L)	Avg. Speed (km/h)	Distance (km)		
11	1	2	1	208.31	117.28	25.62	39.40	65.02	55.00	395.70	237.96	143.38	26.56	41.00	67.56	58.75	409.33		
11	2	2	1	269.73	148.15	33.92	52.93	86.84	56.25	530.61	284.79	165.81	32.49	52.49	84.99	55.42	527.11		
11	3	2	1	254.96	141.09	32.04	49.29	81.33	57.08	493.05	254.96	141.09	32.04	49.29	81.33	57.08	493.05		
11	4	2	1	236.49	132.15	28.67	45.86	74.52	57.50	458.44	247.10	139.19	29.27	47.80	77.08	55.00	480.09		
11				242.37	134.67	30.06	46.87	76.93	56.46	469.45	256.20	147.37	30.09	47.65	77.74	56.56	477.40		
16	1	2	1	319.02	158.81	42.24	72.19	114.43	65.29	656.12	348.12	180.40	47.52	72.28	119.80	60.88	709.14		
16	2	2	1	238.02	121.03	31.91	51.65	83.56	57.35	516.88	238.02	121.03	31.91	51.65	83.56	57.35	516.88		
16	3	3	1	343.04	186.30	42.93	69.03	111.96	55.83	692.55	348.92	187.48	44.10	71.22	115.32	55.83	714.65		
16	4	3	1	262.31	126.14	37.53	59.73	97.26	55.00	599.85	375.62	205.85	46.94	74.32	121.27	55.00	746.44		
16				290.60	148.07	38.65	63.15	101.80	58.37	616.35	327.67	173.69	42.62	67.37	109.99	57.27	671.78		
21	1	3	1	344.47	164.71	50.22	78.18	128.40	55.43	784.46	347.07	167.16	50.56	77.95	128.51	55.00	782.85		
21	2	3	1	308.18	143.58	46.16	71.41	117.57	56.30	715.47	384.67	194.25	53.43	82.59	136.01	55.00	829.41		
21	3	3	1	205.33	98.81	29.88	46.21	76.09	58.26	459.55	208.71	102.78	29.56	46.10	75.66	58.26	458.50		
21	4	3	1	308.73	132.51	50.11	75.76	125.87	55.65	759.63	350.32	166.01	51.76	79.89	131.65	55.00	802.38		
21				291.68	134.90	44.09	67.89	111.98	56.41	679.78	322.69	157.55	46.32	71.63	117.96	55.82	718.28		
Average				274.88	139.21	37.60	59.30	96.91	57.08	588.53	302.19	159.53	39.68	62.22	101.89	56.55	622.49		